2-DIMENSIONAL TRANSLATION INVARIANT RI-SPLINE WAVELET AND ITS APPLICATION

Zhong Zhang, Satoshi Horihata, Tetsuo Miyake

Toyohashi University of Technology
Department of Production System Engineering
1-1 Hibarigaoka, Tempaku-cho,
Toyohashi 441-8580, Japan

Hiroshi Toda

Okayama Prefectural University
Department of Systems Engineering
111 Kuboki, Soja 719-1197 Japan

ABSTRACT

In this study, we propose a 2-dimensional translation invariant Real-Imaginary Spline Wavelet (RI-Spline wavelet) and develop a 2-dimensional Complex Discrete Wavelet Transform (2-D CDWT). The main results obtained can be summarized as follows: 1) The problem of 2-D translation variance which is caused by the DWT using a real mother wavelet can be solved by using the 2-D RI-Spline wavelet. 2) The 2-D RI-Spline wavelet is applied to image processing, and encouraging results are obtained.

1. INTRODUCTION

The Discrete Wavelet Transform (DWT) is a frequency-space analysis method for which a very efficient computation algorithm, the Multi-resolution Analysis (MRA) has been proposed by Mallat[1]. However, the DWT has a translation variance problem[2]. This problem hinders the DWT from being used in wider fields. Currently, successful applications of the DWT are restricted to image compression etc.

In order to overcome this translation variance problem of the DWT, Kingsbury[3] turned his attention to the single phase of a real wavelet causing the lack of shift invariance, and he proposed a pseudo complex wavelet(hereafter, we will call it a complex wavelet), and achieved parallel computation using an algorithm named the Dual-Tree Algorithm for this complex wavelet. However, the major drawback of Kingsbury's approach is that in the process of creating a half-sample-delay, level -1 decomposition results can not be used for complex analysis, although the computational complexity is only twice that of the conventional DWT. So it is difficult to use Kingsbury's method for image processing. On the other hand, Fernandes *et al.* [4] proposed a new framework for the implementation of the Complex Discrete Wavelet Transform (CDWT), in which input data are transformed into a spatial domain in order to obtain a Hilbert pair of input data, and the computational complexity is bigger than that of Kingsbury's method.

To overcome the disadvantage of Kingsbury's method, we have proposed a new complex wavelet, the RI-Spline wavelet and a Coherent Dual-Tree algorithm for the RI-Spline wavelet, in which the half-sample-delay between two parallel trees has been achieved by using interpolation and the complex analysis can be carried out coherently in all analysis levels[5].

In this study, we extend the 1-D RI-Spline wavelet to the 2-D RI-Spline wavelet and develop a 2-D CDWT. The 2-D RI-Spline wavelet is applied to image processing and experimental results using a model image and a medical image de-noising show that, using our method better results can be obtained than that obtained by the traditional 2-D DWT.

2. 2-D RI-SPLINE WAVELET AND THE 2-D CDWT

2.1. 1-D RI-Spline wavelet and CDWT

The RI-Spline wavelet and its scaling functions are defined as follows[5]:

$$\begin{aligned}&\psi(t) = \psi_R(t) + j\psi_I(t),\\ &\quad \psi_R(t) = (-1)^{(m_e-2)/2}||\psi_{m_e}||^{-1}\psi_{m_e}(t+m_e-1),\\ &\quad \psi_I(t) = (-1)^{(m_o+1)/2}||\psi_{m_o}||^{-1}\psi_{m_o}(t+m_o-1),\end{aligned} \tag{1}$$

$$\begin{aligned}N_R(t) &= N_{m_e}(t-m_e/2),\\ N_I(t) &= N_{m_o}(t-(m_o-1)/2),\end{aligned} \tag{2}$$

where $\psi_R(t)$ and $\psi_I(t)$ denote the real and imaginary components of the RI-Spline wavelet, $N_R(t)$ and $N_I(t)$ the real and imaginary components of the RI-Spline scaling function, $\psi_{m_e}(t)$ and $\psi_{m_o}(t)$ the m_o and m_e Spline wavelets, and $N_{m_e}(t)$ and $N_{m_o}(t)$ the m_e and m_o Spline scaling function, and Eqs. (1) and (2) contain the phase adjustment. The normalization of the wavelets is conducted as follows:

$$\begin{aligned}&\langle \psi^j_{R,k}, \psi^j_{I,k}\rangle = 0,\\ &||\psi^j_{R,k}|| = ||\psi^j_{I,k}|| = 1.\end{aligned} \tag{3}$$

After normalizing the decomposition sequences $\{a_k^{m_e}\}$ and $\{b_k^{m_e}\}$ of the m_e Spline wavelet $\psi_{m_e}(t)$, they are used as

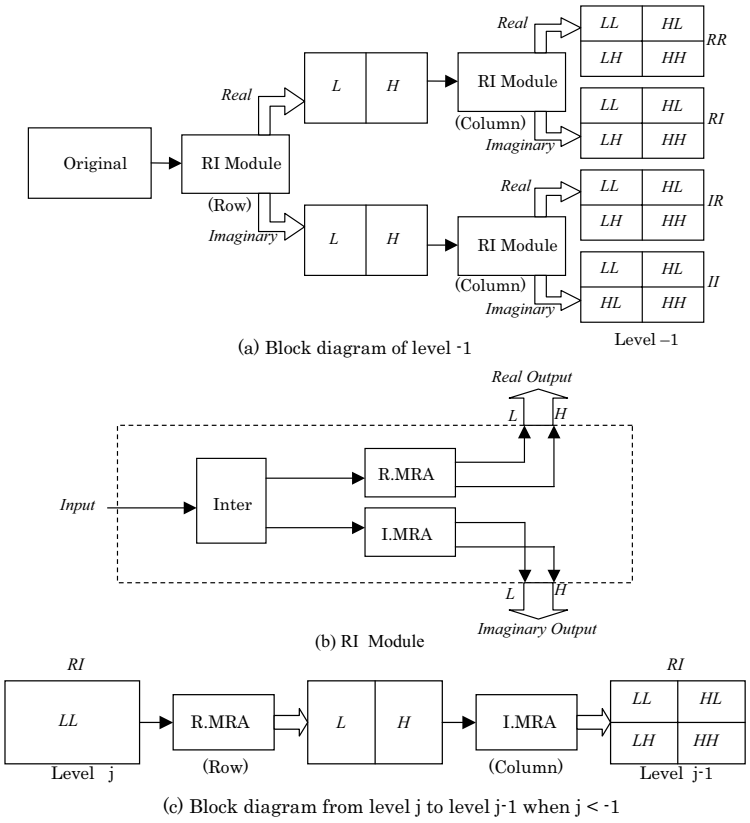

Fig. 1. The 2-D CDWT implementation and module's definition.

the decomposition sequences $\{a_k^R\}$ and $\{b_k^R\}$ of $\psi_R(t)$. The same is true for $\{a_k^I\}$ and $\{b_k^I\}$ of $\psi_I(t)$.

The 1-D CDWT using the RI-Spline wavelet is created by the Coherent Dual-Tree Algorithm (CDTA) which consists of two trees; a real tree and an imaginary tree. In the decomposition trees, the real and imaginary parts of the complex coefficients $d_{R,k}^j$ and $d_{I,k}^j$ are produced. The decomposition trees of the CDTA start from $c_{R,k}^0$ and $c_{I,k}^0$, which are calculated by interpolation using the synthetic-interpolation function and the half-sample-delay between $c_{R,k}^0$ and $c_{I,k}^0$ can be achieved.

We here define a synthetic wavelet $|d_k^j|$ as follows:

$$|d_k^j| = \sqrt{(d_{R,k}^j)^2 + (d_{I,k}^j)^2} \tag{4}$$

Based on Eq.(3), the following relation can be easily obtained.

$$||d_{R,k}^j \psi_{R,k}^j + d_{I,k}^j \psi_{I,k}^j|| = \sqrt{(d_{R,k}^j)^2 + (d_{I,k}^j)^2} \tag{5}$$

Therefore, the synthetic wavelet $|d_k^j|$ can be considered as the norm of wavelet coefficients $d_{R,k}^j$ and $d_{I,k}^j$. So it can be used as a translation invariant feature for its insensitivity to phase.

2.2. Extending the 1–D RI-Spline wavelet and the CDWT to the 2-D

We summarize how the 1–D wavelet and the DWT is extended to the 2–D. First, each row of the input image is subjected to level -1 wavelet decomposition. Then each column of these results is subjected to level -1 wavelet decomposition. In each decomposition, the data is simply decomposed into a high-frequency component (H) and a low-frequency component (L). Therefore, in level -1 decomposition, the input image is divided into HH, HL, LH, and LL components. We denote high-frequency in the row direction and low-frequency in the column direction as HL and so on. The same decomposition is continued recursively for the LL component.

Following this procedure shown above, we extend the 1–D RI-Spline and the CDWT to the 2-D. As shown in Fig.2(a), each row of the input image first is subjected to 1–D RI-spline wavelet decomposition; one is a real decomposition that uses the real component of the RI-spline wavelet and the other is an imaginary decomposition that uses the imaginary component of the RI-spline wavelet. Then each column of these results is also subjected to a 1–D RI-spline wavelet decomposition. In this way, we obtain level -1 decomposition results. When level -1 decomposition is

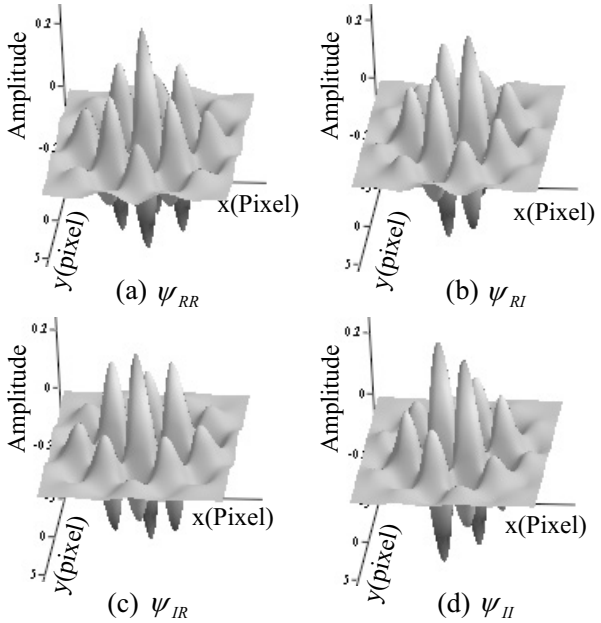

Fig. 2. Example of 2 dimension RI-Spline wavelets.

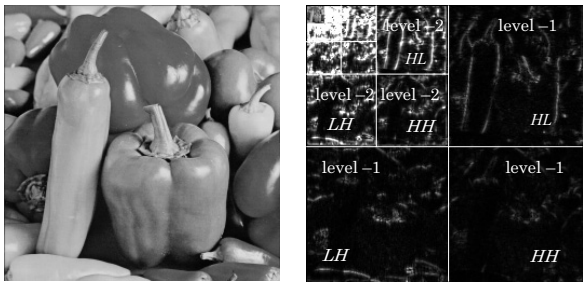

(a) 256X256 Peppers Image (b) Characteristic Image by using RI-Spline wavelet's 2-D CDWT

Fig. 3. Norm obtained by 2-D CDWT using m=4,3 RI-Spline wavelet from level -1 to level -4.

finished, we obtain four times as many results as with the ordinary 2-D DWT decomposition. That is, the 2-D CDWT has 4 decomposition types; RR, RI, IR, and II as shown in Fig. 2(a). We denote a real decomposition in the row direction and an imaginary decomposition in the column direction as RI and so on. Note that each of these decompositions has HH, HL, LH, and LL components in it. Furthermore, for the LL component, the same decomposition by which the LL component has been calculated, is continued recursively as shown in Fig.2(c).

The 2-dimensional RI-Spline wavelet functions of RR, RI, IR, and II can be expressed as follows using 1–D wavelet functions $\psi_R(t)$ and $\psi_I(t)$ [1].

$$\begin{aligned} \psi_{RR}(x,y) &= \psi_R(x)\psi_R(y) \\ \psi_{RI}(x,y) &= \psi_R(x)\psi_I(y) \\ \psi_{IR}(x,y) &= \psi_I(x)\psi_R(y) \\ \psi_{II}(x,y) &= \psi_I(x)\psi_I(y) \end{aligned} \tag{6}$$

Figure 2 shows these 2-D wavelet functions, where Fig. 2(a) shows the wavelet function ψ_{RR}, (b) wavelet function ψ_{IR}, (c) wavelet function ψ_{RI} and (d) wavelet function ψ_{II}. Comparing Fig. 2(a), (b), (c) and (d), it is clear that the wave shape of ψ_{RR}, ψ_{RI}, ψ_{IR} and ψ_{II} are different, so different information can be extracted by using them.

Moreover, based on Eq. (3) and (6), the norm of the 2-D RI-Spline wavelet function ψ^j_{RR} at a point (k_x, k_y) of level j, $||\psi^j_{RR}(x-k_x, y-k_y)||$, which is abbreviated to $||\psi^j_{RR,k_x,k_y}||$ hereafter, can be expressed as follows:

$$\begin{aligned} ||\psi^j_{RR,k_x,k_y}|| &= ||\psi^j_{R,k_x}\psi^j_{R,k_y}||^2 \\ &= ||\psi^j_{R,k_x}||^2||\psi^j_{R,k_y}||^2 \\ &= 1 \end{aligned} \tag{7}$$

The same is true for the other wavelet functions ψ^j_{RI}, ψ^j_{IR} and ψ^j_{II}. Furthermore, the inner product of ψ^j_{RR,k_x,k_y}, ψ^j_{RI,k_x,k_y}, ψ^j_{IR,k_x,k_y}, and ψ^j_{II,k_x,k_y} is zero since $< \psi^j_{R,k}, \psi^j_{I,k} >$=0. This means that the 2-D wavelet functions shown in Eq. (6) are orthogonal to each other. The 2-D synthetic wavelet $|d^j_{k_x,k_y}|$ of the wavelet coefficients in HH of RR, RI, IR, and II that were obtained in level j (k_x, k_y) by the 2-D CDWT using the 2-D RI-Spline can be defined as follows:

$$|d^j_{k_x,k_y}| = \tag{8}$$

$$\sqrt{(d^j_{RR,k_x,k_y})^2 + (d^j_{RI,k_x,k_y})^2 + (d^j_{IR,k_x,k_y})^2 + (d^j_{II,k_x,k_y})^2}$$

As is the same with the 1–D case, the 2-D synthetic wavelet $|d^j_{k_x,k_y}|$ becomes the norm. So it can be treated as a translation invariant feature, because it is insensitive to phase. The same result can be obtained in the case of LH and HL.

Figure 3(b) shows an example of the 2–D synthetic wavelet of the wavelet coefficient from level -1 to level -4 that was obtained by a 2–D RI-Spline wavelet applied to the original image shown as Fig. 3(a). As shown in Fig. 3, it is clear that the 2–D synthetic wavelet in LH, HH, HL carries the intrinsic information on each local point.

3. EXPERIMENTAL DEMONSTRATION OF TRANSLATION INVARIANCE

We perform an experiment to demonstrate the translation invariance of the 2-D RI-Spline wavelet. Fig.4 (a) shows the impulse response of the 2-D m=4 Spline wavelet, and Fig.4 (b) shows the impulse response of the 2-D m=4,3 RI-Spline wavelet. Here, "impulse response" means the following. The input images have "impulse" when only one pixel is 1, and all of the other pixels are 0. Then the horizontal position of the impulse shifts one by one. These "impulse" input images are subjected to a 2-D DWT using the m=4 Spline wavelet and the 2-D CDWT using the

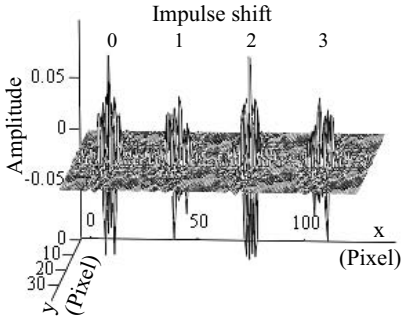

(a)Impulse response of m=4 Spline wavelet

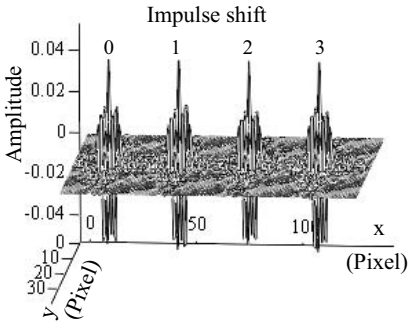

(b)Impulse response of m=4,3 RI-Spline wavelet

Fig. 4. Impulse responses of m=4 Spline wavelet and m=4,3 RI-Spline wavelet on level-2.

m=4,3 RI-Spline wavelet. After subjecting to the 2-D DWT using the m=4 Spline wavelet and the 2-D CDWT using the m=4,3 RI-Spline wavelet, only the coefficients of HH in level -2 are retained, with the other coefficients rewritten to be 0. These coefficients are used for reconstruction by the inverse transform. "Impulse response" means these reconstructed images are overwritten. If the shapes of these "impulse responses" are the same independent of the position of the impulse, the wavelet transform used to make the "impulse response" can be considered to be translation invariant. Comparing Fig.4 (a) with Fig.4 (b), the "impulse response" of the 2-D m=4,3 RI-Spline wavelet has uniform shape while that of the 2-D m=4 Spline wavelet does not.

Fig.5 (a) shows the impulse response energy of the 2-D m=4 Spline wavelet, and Fig.5 (b) shows the impulse response energy of the 2-D m=4,3 RI-Spline wavelet. Here, "impulse response energy" means the square-sum of the coefficients of HH in level -2 obtained from the impulse input. Comparing Fig.5 (a) and (b), it is clear that the impulse response energy of the 2-D RI-Spline wavelet is stable, which means the transform used to make the impulse response energy is translation invariant.

4. APPLICATION FOR IMAGE DE-NOISING

In the 1-D case, the Wavelet Shrinkage has been extended using a translation invariant RI-Soline wavelet in [6]. In this study, the 2-D extension is developed. Our experiments using a model image and a medical image show that our method using the m=4,3 RI-Spline wavelet has better de-noising performance than that of the m=4 spline wavelet and the smoothing filter.

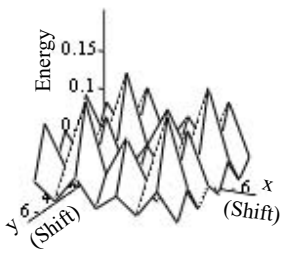

(a)Impulse response energy by m=4 Spline wavelet

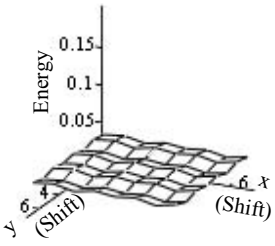

(b) Impulse response energy by m=4,3 RI-Spline wavelet

Fig. 5. Impulse responses energy of m=4 Spline wavelet and m=4,3 RI-Spline wavelet on level-2.

5. CONCLUSIONS

In this study, we extended the 1-D RI-Spline wavelet to the 2-D RI-Spline wavelet and developed the 2-D CDWT using the 2-D RI-Spline wavelet. Translation invariance in the image processing has been achieved by using the 2-D RI-Spline wavelet. Furthermore, the 2-D RI-Spline wavelet was applied to image processing and experimental results using a model image and a medical image de-noising show that by using our method better results can be obtained than that obtained by the traditional 2-D DWT.

6. REFERENCES

[1] S. Mallat, "A theory for Multiresolution Signal Decomposition: The Wavelet Representation," IEEE Trans. on Pattern Analysis and Machine Intelligence, **11**-7, 1989, 674-693.

[2] S. Mallat, a wavelet tour of signal processing, Academic Press, 1999, 146

[3] N. Kingsbury, "Complex Wavelets for translation invariant analysis and filtering of signals," *Journal of Applied and Computational Harmonic Analysis*, **10**–3, May 2001, 234-253.

[4] F. C. A. Fernandes *et al.*, "Complex wavelet transforms with allpass filters,"*Signal Processing,* **88**–8, 2003, 1689-1706.

[5] Z. Zhang, H. Fujiwara, H. Toda and H. Kawabata, "A New Complex Wavelet Transform by Using RI-Spline Wavelet, " Pro. ICASSP 2004, II, 937-940.

[6] Z. Zhang, H. Fujiwara, and Fuji Ren, "Signal Processing Using Translation Invariant RI-Spline Wavelet, " Proc. IEEE SMC 2004.